

## Preparation of Nano-Size Al-Promoted Sulfated Zirconia and the Impact of Calcination Temperature on Its Catalytic Activity

B. R. Vahid,<sup>a</sup> N. Saghatoleslami,<sup>a,\*</sup> H. Nayebzadeh,<sup>a</sup> and A. Maskooki<sup>b</sup>

<sup>a</sup>Department of Chemical Engineering, Ferdowsi University of Mashhad, Mashhad, Iran

<sup>b</sup>Department of Food Technology, Khorasan Research Institute for Food Science and Technology, Mashhad, Iran

Original scientific paper

Received: January 19, 2012

Accepted: May 21, 2012

Solvent-free technique was employed in this work in order to assess the influence of the calcination temperature on the activity of Al-promoted sulfated zirconia. The catalyst was analyzed by XRD and IR-spectrum method, and catalytic activity was examined by esterification reaction of oleic acid. XRD analysis revealed that a decline in the percentage of tetragonal phases of zirconia was observed by increasing the calcination temperature from 500 to 900 °C. In addition, a reduction of sulfate groups as  $\text{SO}_4^{2-}$  on zirconia surface was observed. As a consequence, a decline in Brønsted sites with calcination temperature enhancement also prevailed. Therefore, the size of Al-promoted sulfated zirconia particles was increased accordingly. On the other hand, with the aluminum sulfate loading, the amount of sulfate ions on Al-promoted sulfated zirconia surface was enhanced and a reduction in particle size of  $\text{Al}_2\text{O}_3/\text{S-ZrO}_2$  was also observed, as compared to non-promoted. The result of this study revealed that an increase of sulfate and alumina groups causes a raise in the acidity of catalyst. Furthermore, the calcined Al-promoted and non-promoted sulfated zirconia would convert 96.10 % and 89.36 % of oleic acid to biodiesel, respectively. Therefore,  $\text{Al}_2\text{O}_3/\text{S-ZrO}_2$  as a catalyst exhibits a higher activity than  $\text{S-ZrO}_2$ .

*Key words:*

Sulfated zirconia, alumina, solvent-free, calcination, esterification

### Introduction

In the last decade, scientists have looked for an alternative to fossil fuels due to their environmental impacts, limited resources, and considerable price increases. Biodiesel, a transesterified product of vegetable oil, is considered the most promising for substituting diesel fuel. Biodiesel is a green fuel that does not enhance the greenhouse effect and global warming.<sup>1</sup>

Biodiesel fuel is produced by transesterification of triglycerides (virgin vegetable oil) with a short chain alcohol in the presence of catalyst.<sup>2,3</sup> However, virgin vegetable oil renders biodiesel production costly. In fact, 60–80 % of biodiesel-production costs greatly depends upon the feedstock prices.<sup>4</sup> Therefore, low-quality feedstock such as inedible oil, waste cooking oil and inedible animal fats could be a good feedstock for the reaction. Moreover, utilization of waste cooking oil for the reaction would significantly reduce the problem of waste-oil disposal.<sup>5–7</sup> However, waste cooking oil has a dramatically high percentage of free fatty acid (FFA). This is an unfavorable feature in the conven-

tional method of biodiesel production with base homogeneous catalysts such as NaOH and KOH. The reaction between FFA and base catalysts produces soap as a by-product. Subsequently, the final product requires the expensive step of separating and purifying the biodiesel from the product and by-product mixture. This process causes a reduction in the FAME yield.<sup>8,9</sup> Hence, before the transesterification reaction with alkaline homogeneous catalysts, FFA must be converted to methyl ester with esterification reaction. Traditionally, acidic homogeneous catalysts such as sulfuric acid or hydrochloric acid, are used for the esterification reaction. However, utilization of acidic catalysts has a high corrosive effect, causing environmental problems. Furthermore, the reaction requires a higher temperature and alcohol/oil mole ratio, thus implying a longer time for the reaction to proceed.<sup>10,11</sup> Therefore, utilization of solid acid catalysts instead of acidic homogeneous catalysts is proposed. These catalysts are usually not as problematic as the conventional acid catalysts, and are simply separated from the mixture product by filtration. The most notable advantage of biodiesel production with heterogeneous catalysts is their lengthened lifetime in

\*Corresponding author: slami@um.ac.ir; Tel/fax: (+98) 511 8816840

subsequence reactions.<sup>12–18</sup> Recently, many solid acid catalysts such as earth metal oxides have also been investigated by researchers.<sup>19–22</sup>

Among these catalysts,  $\text{SO}_4^{2-}/\text{ZrO}_2$  exhibit a higher activity and acidity for the esterification and the transesterification reaction.<sup>23–26</sup> Nevertheless, S-ZrO<sub>2</sub> shows considerable activity losses with subsequent reaction cycles.<sup>27</sup> Therefore, other metal oxides are also employed to modify the structure of this catalyst and improve its properties.<sup>28–32</sup> However, the activity and acidity of the catalyst are an important criterion in the preparation methods for them. These catalysts are generally prepared by co-precipitation,<sup>21–31</sup> impregnation,<sup>32–34</sup> and solvent-free methods.<sup>35</sup> Sun *et al.* investigated the properties of Al-promoted and non-promoted sulfated zirconia and showed that the Al-promoted sulfated zirconia has higher surface area, catalytic activity and stability.<sup>36</sup> It is also worth mentioning that calcination temperature is an important parameter in the activity of catalysts.<sup>37</sup> Ramu *et al.* investigated the effect of calcination temperature on activity of the prepared  $\text{WO}_3/\text{ZrO}_2$  catalysts by impregnation and co-precipitation method. They reported that the calcined catalysts at 500 °C exhibit the highest activity for the esterification of palmitic acid.<sup>38</sup>

Therefore, it is the aim of this work to examine the influence of calcination temperature on the activity and acidity of  $\text{Al}_2\text{O}_3/\text{S-ZrO}_2$  in the esterification of oleic acid to FAME (biodiesel).

## Material and methods

### Catalysts preparation

$\text{Al}_2\text{O}_3/\text{S-ZrO}_2$  was prepared by solvent-free method. To attain this objective,  $\text{ZrOCl}_2 \cdot 8\text{H}_2\text{O}$ ,  $(\text{NH}_4)_2\text{SO}_4$  (molar ratio 1:6) and  $\text{Al}_2(\text{SO}_4)_3 \cdot 18\text{H}_2\text{O}$  (molar ratio 1 : 0.2 as 3 mol. % of  $\text{Al}_2\text{O}_3$ ) was mixed in a porcelain mortar for 20 minutes at room temperature. Then, the samples kept at room temperature for 18 hrs, and were calcined for 5 hrs at temperatures ranging from 500 to 900 °C.<sup>36</sup>

### Catalyst characterizations

Phase identification and crystalline size of the modified sulfated-zirconia were determined by X-ray diffraction method by means of  $\text{Cu K}\alpha$  radiation ( $\lambda = 1.5406 \text{ \AA}$ ) at 45 kV and 80 mA, over a  $2\theta$  ranging from 20 to 70° at a scanning speed of 10°/min. The crystalline size of tetragonal and monoclinic phases was computed by Scherrer's equation as shown below:<sup>39,40</sup>

$$D = 0.9\lambda/\beta \cos \theta \quad (1)$$

where  $D$  is the crystalline size in nm,  $\lambda$  is the radiation wavelength,  $\beta$  is the corrected half-width of the peak profile, and  $\theta$  is the corrected half-width of the diffraction peak angle.

The phases were distinguished using infrared (IR) spectra recorded on a spectrometer in the range of 600–4000  $\text{cm}^{-1}$  and the standard KBr technique was utilized for the sample preparation.

Then the catalysts acidity was evaluated by titration of 0.2 g solution of the catalyst in 10 mL of deionized water. For the next step, the mixtures were titrated with 0.1 mol  $\text{L}^{-1}$  aqueous solution of NaOH using phenolphthalein as an indicator. This was accomplished in accordance with the aqueous ion-exchange of the catalyst  $\text{H}^+$  with  $\text{Na}^+$  ions.<sup>41</sup>

### Catalysts activity

Activity of the catalysts was examined from the esterification reaction between oleic acid and methanol. The reaction was carried out in an 80 mL stainless steel autoclave. The reaction was executed containing 10 g oleic acid, 12.9 mL methanol and 0.3 g of the catalyst at 90 °C for 30 min and stirred at 600 rpm. The authors usually performed reaction in alcohol boiling point. However, this takes more time for reaction completion.<sup>33</sup> Therefore, the reaction time was reduced by increasing of reaction temperature.<sup>11</sup> Although, the reaction conditions were not optimized for the highest reaction yield, they provided a way to compare the activities of the catalysts. Afterwards, in order to separate the catalyst and the excess methanol, the product was filtered and vaporized. Finally, the conversion of oleic acid to methyl ester was calculated from the following equation:<sup>27–42</sup>

$$AV = N \cdot M_w \cdot V/m \quad (2)$$

$$\begin{aligned} \text{Conversion percentage (\%)} &= \\ &= 100 \cdot (AV_{\text{Oleic acid}} - AV_{\text{Methyl Ester}})/AV_{\text{oleic acid}} \end{aligned} \quad (3)$$

where AV is the acid value, N is the normality of KOH-ethanol solution (0.1 mol  $\text{m}^{-3}$ ), m (g) is the mass of the sample and  $M_w$  is the molecular mass of the KOH and  $V$  ( $\text{cm}^3$ ) is the volume of KOH-ethanol solution employed for titration.

## Results and discussions

### XRD analysis

The XRD pattern for four calcined samples at various calcination temperature is shown in Fig. 1. For the calcined catalyst at 500 °C, two peaks of tetragonal phases of zirconia at  $2\theta = 30.3^\circ$  and  $50.4^\circ$  and two small peak of monoclinic phases of

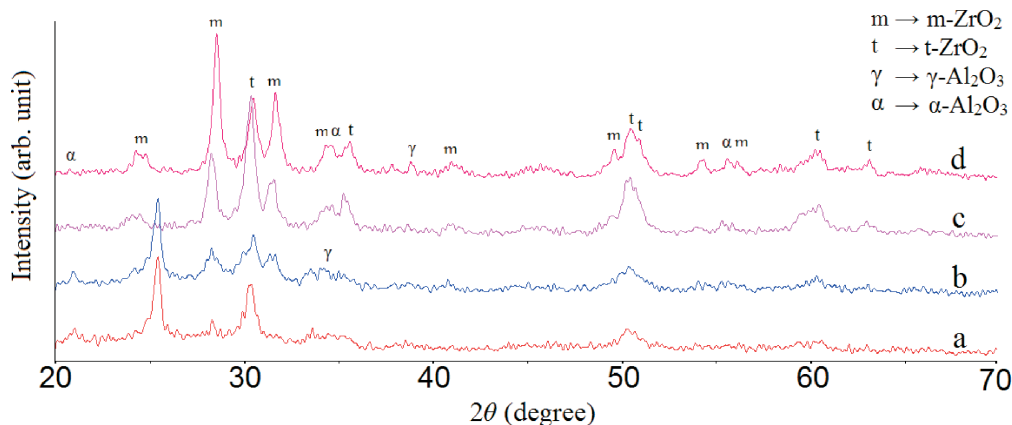


Fig. 1 – XRD pattern for 3 mol. % of  $\text{Al}_2\text{O}_3/\text{S-ZrO}_2$  calcined at a) 500 °C, b) 600 °C, c) 700 °C and d) 900 °C

zirconia at  $2\theta = 28.2^\circ$  and  $33.5^\circ$  were observed. As the Fig. 1 illustrates, a raise in the calcination temperature causes the formation of monoclinic phases of zirconia. However, for the calcined catalyst at 600 °C, monoclinic phases of zirconia was also observed at  $2\theta = 24.2^\circ$ ,  $31.5^\circ$ ,  $41^\circ$ ,  $54.1^\circ$  and  $55.7^\circ$  and  $2\theta = 28.2^\circ$  and  $33.5^\circ$ . A new weak peak of tetragonal phase of zirconia was also formed at  $2\theta = 60^\circ$ .<sup>43</sup> Furthermore, tetragonal peaks of zirconia have also been observed at  $2\theta = 35.4^\circ$  and  $63.1^\circ$ , where the height of monoclinic and tetragonal phase peaks increases sharply with the calcination temperature up to 700 °C. A further increase in the calcinations temperature causes the height of the peaks of monoclinic and tetragonal phase increases accordingly.

As shown in Fig. 1, the areas under the curves for tetragonal phases are less than those of monoclinic phases. Monoclinic phase was fully developed while increasing the calcination temperature from 700 to 900 °C since an observation of its perfectly separated peak apparently occurred at  $2\theta = 50.4^\circ$ . Furthermore, a decrease in the area of tetragonal phases in comparison with monoclinic phases of zirconia was also observed.<sup>18</sup> In this work, fractional conversion of tetragonal phases in the catalysts was calculated by the following formula as suggested by Valigi *et al.*<sup>44</sup>

$$f_t = A_t(101)/A_{\text{total}}(\text{ZrO}_2) \quad (4)$$

where  $f_t$  is the fraction of tetragonal phase,  $A_t(101)$  is the peak area of (101) of tetragonal phases and  $A_{\text{total}}(\text{ZrO}_2)$  is the area of all tetragonal and monoclinic peaks in the pattern.

Table 1 presents the percentage of tetragonal phases and activity of the catalysts in the esterification reaction of oleic acid. Table 1 illustrates the conversions of oleic acid by calcined catalysts at various temperatures.

Ramu *et al.* reported that the catalysts activity is linearly proportional to the percentage of tetragonal phases of zirconia. Fig. 2 shows a relationship between the percentage of tetragonal phases and the activity of catalysts in the esterification reaction. This could be caused due to the formation of stable monoclinic phases of zirconia and an increase or a reduction in the area underneath the curve for monoclinic and tetragonal phases in calcination temperature up to 500 °C, respectively. These reasons could significantly reduce the activity of the catalysts. Moreover, the first phases of  $\gamma\text{-Al}_2\text{O}_3$  has also been developed at  $2\theta = 20.9^\circ$  and  $34.5^\circ$  and the peaks for  $\alpha\text{-Al}_2\text{O}_3$  were also detected in the calcinations temperature up to 600 °C. A further increase in the calcination temperature from 600 to 700 °C causes the transformation of  $\gamma \rightarrow \alpha$

Table 1 – Fractional conversion of tetragonal phases and the crystalline size for 3 mol. %  $\text{Al}_2\text{O}_3/\text{S-ZrO}_2$ , at different calcined temperatures

Calcination temperature (°C)	Tetragonal phases (%)	Crystalline size (nm)			Conversion (%)
		tetragonal phases	monoclinic phases	material size	
500	87	7.6	9.5	10.1	96.10
600	60.8	8.2	11.4	12.6	58.49
700	45.2	10.7	14.1	15.4	42.25
900	29.6	10.9	14.7	16	19.18

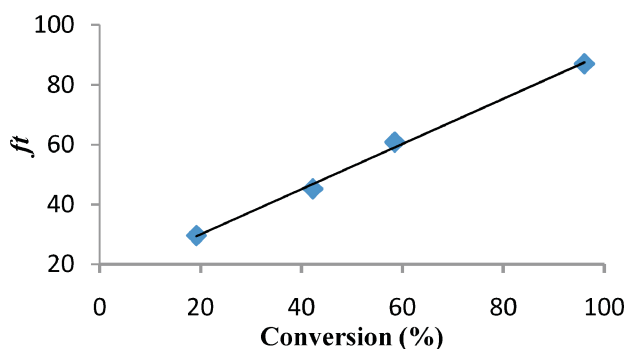


Fig. 2 – Variation of the tetragonal phases of the catalyst with the conversion of oleic acid for 3 mol. % of  $\text{Al}_2\text{O}_3/\text{S-ZrO}_2$  calcined at different temperatures

alumina phase at  $2\theta = 34.5^\circ$ .<sup>45</sup> This transformation could cause a more stable alumina phases. Additional increase in the calcination temperature probably causes the new formation of  $\gamma\text{-Al}_2\text{O}_3$  and  $\alpha\text{-Al}_2\text{O}_3$  phases at  $2\theta = 38^\circ$  and  $55.3^\circ$ , respectively.<sup>19–22,45</sup>

As shown in Fig. 1, the peak at  $2\theta = 25.6^\circ$  was also observed for the calcined catalysts at 500 and 600 °C which denoted the type of crystals of the alumina. Boz *et al.* reported that alumina could not on its own convert the canola oil.<sup>34</sup> This result is in good agreement with the findings of Xie *et al.* cited in the literature.<sup>46</sup> As illustrated in Table 1, the conversion of oleic acid with calcined catalyst at 500 °C is much higher than other calcined catalysts. On the other hand, the calcined catalysts at 600 and 700 °C was only exhibited 58.49 and 42.25 %, respectively. The results of this study also revealed that discrepancy between yields of esterification

reaction for calcined catalyst at 500 and 600 °C whereas both have  $\text{Al}_2(\text{SO}_4)_3$  is much higher than calcined catalyst at 600 and 700 °C. Therefore, the existence of the raw material such as  $\text{Al}_2(\text{SO}_4)_3$  could have a slight or no effect on the activity of the catalysts.

Furthermore, a further increase in calcination temperature would cause a growth in the  $\text{Al}_2\text{O}_3/\text{S-ZrO}_2$  crystalline size from 5 to 25 nm where minimum average size of calcined catalyst at 500 °C was about 10 nm. The formation monoclinic phases of zirconia and transformation of  $\gamma \rightarrow \alpha$  alumina causes the enhancement of the crystalline sizes.

### IR spectral analyses

Fig. 3 shows the IR spectra synthesis of nano-catalysts at various calcination temperature. Paglia *et al.* reported that Al–O stretching vibration of octahedral ( $\text{AlO}_6$ ) and tetrahedral ( $\text{AlO}_4$ ) appears in the range of 500–700 and 700–900  $\text{cm}^{-1}$ , respectively.<sup>47,48</sup> As Fig. 3 demonstrates, the peaks of Al–O stretching vibration could be observed at 680 and 740  $\text{cm}^{-1}$ . Moreover, an additional stretching vibration of Al–O was also formed at 810 and 872  $\text{cm}^{-1}$ .<sup>49</sup> It was also demonstrated that the alumina bands for the calcined catalyst were altered from broad peak at 680–900, and 500 and 600 °C to discrete peak at 700 and 900 °C, respectively. As explained earlier, the alumina group appears at high calcinations temperature. As shown in Fig. 3, the weak bands of alumina groups with sulfate and zirconia groups could have a considerable effect on the enhancement of the activity of catalysts. Fur-

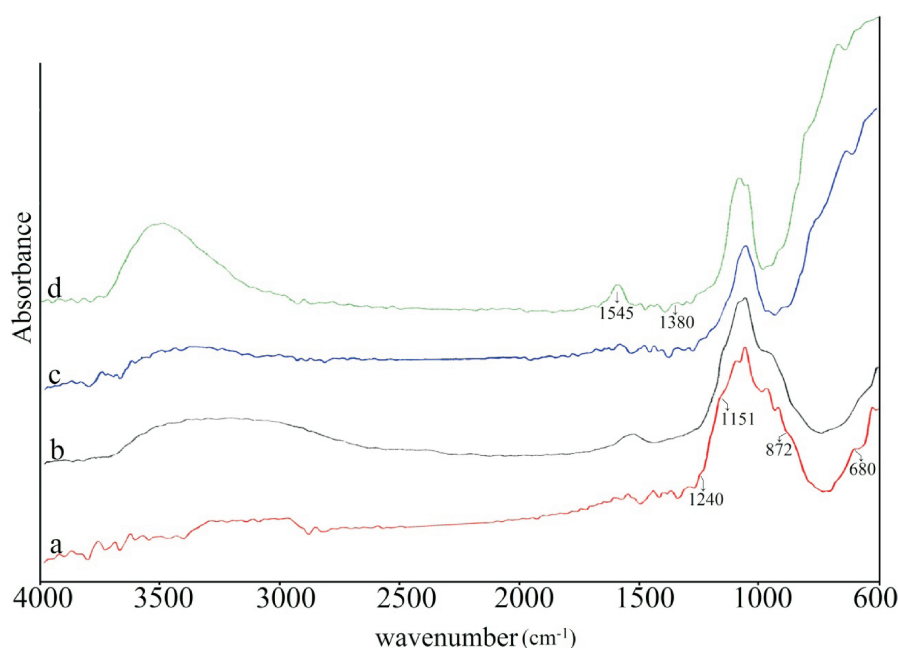


Fig. 3 – Infra-red spectrum of the calcined  $\text{Al}_2\text{O}_3/\text{S-ZrO}_2$  nano crystals at a) 500 °C b) 600 °C c) 700 °C and d) 900 °C



Table 2 – Acidity and activity of SrO/S-ZrO<sub>2</sub> synthesis at different calcination temperature

Catalyst	Calcination temperature (°C)	Tetragonal phases (%)	Acidity (mmol NaOH g <sup>-1</sup> cat)	Conversion (%)
S-ZrO <sub>2</sub>	500	–	4.5	89.36
Al <sub>2</sub> O <sub>3</sub> /S-ZrO <sub>2</sub>	500	87	10.4	96.10
Al <sub>2</sub> O <sub>3</sub> /S-ZrO <sub>2</sub>	600	60.8	2.6	58.49
Al <sub>2</sub> O <sub>3</sub> /S-ZrO <sub>2</sub>	700	45.2	1.2	42.25
Al <sub>2</sub> O <sub>3</sub> /S-ZrO <sub>2</sub>	900	29.6	0.5	19.18

thermore, the stretching vibration bands of X–Al=O was also observed at 980 and 1075 cm<sup>-1</sup>,<sup>50</sup> where the bands adjacent to Al–O were of negligible amount with the enhancement of calcination temperature. Moreover, the decomposition of X–Al=O and formation of two shapes of Al–O were also observed.<sup>51</sup> It could be concluded that the alumina phases became more stable with the separation of X. Therefore, it was apparent that X was the sulfate ions. It is worth mentioning that the sulfate groups had an immense effect on the acidity and activity of the catalysts. It is known that the stretching vibration band of S=O appears at 1100 cm<sup>-1</sup>.<sup>43</sup> Therefore, the weak band appears at 1380 at 1438 cm<sup>-1</sup> which signifies the presence of the SO<sub>3</sub>.<sup>23–52,53</sup> A further increase in the calcination temperature causes the disappearance of weak peak of sulfate groups at 1100 cm<sup>-1</sup>. The finding of this work suggests that an increase in the calcination temperature will lead to the decomposition of sulfate ions on the catalysts. Hence, the decomposition of sulfate ions on the catalysts results in the formation of SO<sub>3</sub> which essentially occurs at higher calcination temperature.<sup>54</sup>

The result of this work also demonstrates that the catalysts exhibit a new band at 1008 cm<sup>-1</sup> at 900 °C. This band alongside with the bands at 1151, and 1240 cm<sup>-1</sup> are normally stands for chelating bidentate sulfate ions coordinated to the zirconium cation.<sup>35,55</sup> The peak of t-ZrO<sub>2</sub> has also been observed at 628 cm<sup>-1</sup>.<sup>43</sup> This peak gradually became weak with intensification in the calcination temperature due to the drop of the fraction of tetragonal phases of zirconia. In addition to these bands, a broad peak of stretching vibration of O–H in the range of 3000–3500 and the bending vibration bands of water were also observed at 1640 and 1660 cm<sup>-1</sup>.<sup>56</sup> It has also been illustrated that a band of O–H has also been observed due to the reaction between air moisture and the catalysts.

Therefore, the bands at 1545 and 1455 cm<sup>-1</sup> could be assigned to Brønsted and Lewis acid sites, respectively, whereas the band at 1495 cm<sup>-1</sup> is normally assigned to a combination band associated with both Brønsted and Lewis acid sites.<sup>57,58</sup>

### Catalysts acidity

Table 2 demonstrates the acidity and activity of the catalysts. The Al<sub>2</sub>O<sub>3</sub>/S-ZrO<sub>2</sub> at 500 °C exhibits a highest acidity, which in turn enhances the catalytic performance. The acidity of catalyst significantly decreases with the enhancement of the calcination temperature to 600 °C. However, the rate of acidity drops significantly with increasing calcination temperature.

As demonstrated earlier and by raising the temperature, either a drop in the percentage of tetragonal phases, decomposition of sulfate ions of the catalysts, a reduction in the amount of sulfate ions on the catalysts surface or the transformation of  $\gamma$ -Al<sub>2</sub>O<sub>3</sub> to stable  $\alpha$ -Al<sub>2</sub>O<sub>3</sub> crystals could cause a reduction in the activity of the catalysts. The relationship between the acidity and activity of catalysts in the esterification reaction are shown in Fig. 4. It also reveals that the activity of the catalysts is roughly exponential and the sharp drop in the acidity of the catalysts could have been caused by the reduction of the sulfate ions and tetragonal phases of zirconia.

As Table 2 demonstrates, 3 mol % of the Al<sub>2</sub>O<sub>3</sub>/S-ZrO<sub>2</sub> at 500 °C exhibits higher acidity and activity than S-ZrO<sub>2</sub>. It could be caused due to the fact that an increase in the sulfated ions on zirconia surface reduces the particle sizes.<sup>36</sup> In addition to sulfated groups, the alumina as a solid acid catalyst also enhances the acidic sites of sulfated zirconia, as the acidity increase from 4.5 to 10.4 mmol

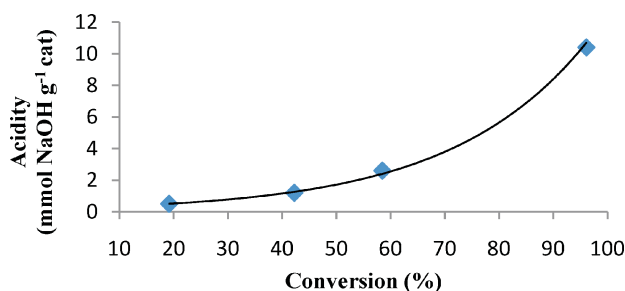


Fig. 4 – Variations of the acidity with activity of the calcined Al<sub>2</sub>O<sub>3</sub>/S-ZrO<sub>2</sub> at different calcinations temperature in the esterification

NaOH g<sup>-1</sup> cat. Thus, the activity of catalyst would enhance the esterification of oleic acid to biodiesel.

## Conclusion

In this work, the impact of calcination temperature in the preparation of Al-promoted sulfated zirconia catalysts was examined by solvent-free method. The finding of this study has revealed that the calcined catalyst at 500 °C enhances the acidity and activity. The sulfate ions have also been decomposed from the catalyst surface by the enhancement in the calcination temperature, which in turn would be converted to SO<sub>3</sub>. The transformation of  $\gamma \rightarrow \alpha$  of Al<sub>2</sub>O<sub>3</sub> has also been carried out by the enhancement of calcination temperature. It has also been demonstrated that the activity of catalysts drops sharply at a higher calcination temperatures and Al-promoted sulfated zirconia exhibits a higher activity than non-promoted sulfated zirconia. The findings of this study also reveal that Al<sub>2</sub>O<sub>3</sub>/S-ZrO<sub>2</sub> at 500 °C could convert 96.1 % of oleic acid to FAME, while S-ZrO<sub>2</sub> only converts 89.36 % of oleic acid under the same condition. It has also been demonstrated that the loaded sulfate and alumina groups on the Al<sub>2</sub>(SO<sub>4</sub>)<sub>3</sub> would enhance the catalytic activity of sulfated zirconia.

## ACKNOWLEDGMENTS

The authors gratefully acknowledge the help of Mr. Mohammadi, technician in the Khorasan Research Institute for Food Science and Technology.

## Nomenclature

- $A_t$  (101) – peak area of (101) of tetragonal phases  
 $A_{\text{total}}$  (ZrO<sub>2</sub>) – area of all tetragonal and monoclinic peaks in the pattern  
 AV – acid value  
 D – crystalline size, nm  
 FFA – free fatty acid  
 $f_t$  – fraction of tetragonal phase  
 IR – Infrared spectroscopy  
 $M_w$  – molecular mass, g mol<sup>-1</sup>  
 N – normality, mol m<sup>-3</sup>  
 V – volume, cm<sup>3</sup>  
 XRD – X-ray diffraction method

## Greek letters

- $\beta$  – the corrected half-width of the peak profile  
 $\lambda$  – the radiation wavelength  
 $\theta$  – the corrected half-width of the diffraction peak angle

## References

- Vyas, A. P., Subrahmanyam, N., Patel, P. A., *Fuel* **88** (2009) 625.
- Boz, N., Kara, M., *Chem. Eng. Commun.* **196** (2008) 80.
- Gerpen, J. V., *Fuel Process. Technol.* **86** (2005) 1097.
- Glisic, S., Lukic, I., Skala, D., *Bioresour. Technol.* **100** (2009) 6347.
- Zhang, Y., Dubé, M. A., McLean, D. D., Kates, M., *Bioresour. Technol.* **89** (2003) 1.
- Demirbas, A., *Energ. Convers. Manage.* **50** (2009) 14.
- Wen, Z., Yu, X., Tu, S.-T., Yan, J., Dahlquist, E., *Bioresour. Technol.* **101** (2010) 9570.
- Lam, M. K., Lee, K. T., Mohamed, A. R., *Appl. Catal. B* **93** (2009) 134.
- Kiss, A. A., Dimian, A. C., Rothenberg, G., *Adv. Synth. Catal.* **348** (2006) 75.
- Lou, W.-Y., Zong, M.-H., Duan, Z.-Q., *Bioresour. Technol.* **99** (2008) 8752.
- Lotero, E., Liu, Y., Lopez, D. E., Suwannakarn, K., Bruce, D. A., Goodwin, J. G., *Ind. Eng. Chem. Res.* **44** (2005) 5353.
- Yan, S., DiMaggio, C., Mohan, S., Kim, M., Salley, S., Ng, K., *Top. in Catal.* **53** (2010) 721.
- Mello, V. M., Pousa, G. P. A. G., Pereira, M. S. C., Dias, I. M., Suarez, P. A. Z., *Fuel Process. Technol.* **92** (2011) 53.
- Wei, Z. B., Yan, W., Zhang, H., Ren, T., Xin, Q., Li, Z., *Appl. Catal. A.* **167** (1998) 39.
- Zabeti, M., Daud, W. M. A. W., Aroua, M. K., *Fuel Process. Technol.* **91** (2010) 243.
- Park, Y.-M., Chung, S.-H., Eom, H. J., Lee, J.-S., Lee, K.-Y., *Bioresour. Technol.* **101** (2010) 6589.
- Sree, R., Seshu Babu, N., Sai Prasad, P. S., Lingaiah, N., *Fuel Process. Technol.* **90** (2009) 152.
- Mongkolbovornkij, P., Champreda, V., Sutthisripok, W., Laosiripojana, N., *Fuel Process. Technol.* **91** (2010) 1510.
- Chen, Y.-H., Huang, Y.-H., Lin, R.-H., Shang, N.-C., Chang, C.-Y., Chang, C.-C., Chiang, P.-C., Hu, C.-Y., J. Taiwan Inst. Chem. Eng. **42** (2011) 937.
- Senso, N., Jongsomjit, B., Praserttham, P., *Fuel Process. Technol.* **92** (2011) 1537.
- Yan, S., Salley, S. O., Simon Ng, K. Y., *Appl. Catal., A.* **353** (2009) 203.
- Sankaranarayanan, T. M., Pandurangan, A., Banu, M., Sivasanker, S., *Appl. Catal., A.* **409** (2011) 239.
- Fu, B., Gao, L., Niu, L., Wei, R., Xiao, G., *Energy Fuels* **23** (2008) 569.
- López, D. E., Goodwin Jr, J. G., Bruce, D. A., Furuta, S., *Appl. Catal. A.* **339** (2008) 76.
- Jitputti, J., Kitiyanan, B., Rangsunvigit, P., Bunyakiat, K., Attanatho, L., Jenvanitpanjakul, P., *Chem. Eng. J.* **116** (2006) 61.
- Rattanaphra, D., Harvey, A. P., Thanapimmetha, A., Srinophakun, P., *Renew. Energy.* **36** (2011) 2679.
- Park, Y.-M., Lee, D.-W., Kim, D.-K., Lee, J.-S., Lee, K.-Y., *Catal. Today* **131** (2008) 238.
- Reddy, B. M., Reddy, G. K., Rao, K. N., Katta, L., *J. Mol. Catal. A: Chem.* **306** (2009) 62.
- Hwang, C.-C., Mou, C.-Y., *J. Phys. Chem.* **113** (2009) 5212.
- Li, Y., Zhang, X.-D., Sun, L., Xu, M., Zhou, W.-G., Liang, X.-H., *Appl. Energy.* **87** (2010) 2369.
- Wang, J., Ma, H., Wang, B., *J. Hazard. Mater.* **157** (2008) 237.
- Chen, X. R., Ju, Y. H., Mou, C. Y., *J. Phys. Chem.* **111** (2007) 731.

33. Wongmaneevil, P., Jongsomjit, B., Praserttham, P., *Catal. Commun.* **10** (2009) 1079.
34. Boz, N., Degirmenbasi, N., Kalyon, D. M., *Appl. Catal. B.* **89** (2009) 590.
35. Garcia, C. M., Teixeira, S., Marciniuk, L. L., Schuchardt, U., *Bioresour. Technol.* **99** (2008) 6608.
36. Sun, Y., Ma, S., Du, Y., Yuan, L., Wang, S., Yang, J., Deng, F., Xiao, F.-S., *J. Phys. Chem. B.* **109** (2005) 2567.
37. Yee, K. F., Wu, J. C. S., Lee, K. T., *Biomass Bioenergy* **35** (2011) 1739.
38. Ramu, S., Lingaiah, N., Prabhavathi Devi, B. L. A., Prasad, R. B. N., Suryanarayana, I., Sai Prasad, P. S., *Appl. Catal. A* **276** (2004) 163.
39. Kongwudthiti, S., Praserttham, P., Inoue, M., Tanakulrungsank, W., *J. Mater. Sci. Lett.* **21** (2002) 1461.
40. Kongwudthiti, S., Praserttham, P., Tanakulrungsank, W., Inoue, M., *J. Mater. Process. Technol.* **136** (2003) 186.
41. López, D. E., Suwannakarn, K., Bruce, D. A., Goodwin Jr, J. G., *J. Catal.* **247** (2007) 43.
42. Kim, H.-J., Kang, B.-S., Kim, M.-J., Kim, D.-K., Lee, J.-S., Lee, K.-Y., *Stud. Surf. Sci. Catal.* **153** (2004) 201.
43. Niu, L., Gao, L., Xiao, G., Fu, B., *Asia-Pacific J. Chem. Eng.* **7** (2012) 222.
44. Valigi, M., Gazzoli, D., Pettiti, I., Mattei, G., Colonna, S., De Rossi, S., Ferraris, G., *Appl. Catal. A* **231** (2002) 159.
45. Cava, S., Tebcherani, S. M., Souza, I. A., Pianaro, S. A., Paskocimas, C. A., Longo, E., Varella, J. A., *Mater. Chem. Phys.* **103** (2007) 394.
46. Xie, W., Li, H., *J. Mol. Catal. A: Chem.* **255** (2006) 1.
47. Lukić, I., Krstić, J., Jovanović, D., Skala, D., *Bioresour. Technol.* **100** (2009) 4690.
48. Paglia, G., Buckley, C. E., Udovic, T. J., Rohl, A. L., Jones, F., Maitland, C. F., Connolly, J., *Chem. Mater.* **16** (2004) 1914.
49. Xu, C., Sun, J., Zhao, B., Liu, Q., *Appl. Catal. B* **99** (2010) 111.
50. Ram, S., Rana, S., *Materials Letters* **42** (2000) 52.
51. Ram, S., Singh, T. B., Pathak, L. C., *Phys. Status Solidi.* **165** (1998) 151.
52. Li, X. B., Nagaoka, K., Simon, L. J., Olindo, R., Lercher, J. A., Hofmann, A., Sauer, J., *J. Am. Chem. Soc.* **127** (2005) 16159.
53. Sun, Y. Y., Ma, S. Q., Du, Y. C., *J. Phys. Chem. B.* **109** (2005) 2567.
54. Funamoto, T., Nakagawa, T., Segawa, K., *Appl. Catal. A* **286** (2005) 79.
55. Valigi, M., Gazzoli, D., Pettiti, I., Mattei, G., Colonna, S., De Rossi, S., Ferraris, G., *Appl. Catal. A* **231** (2002) 159.
56. Babou, F., Coudurier, G., Vadrine, J. C., *J. Catal.* **152** (1995) 341.
57. Chen, X.-R., Ju, Y.-H., Mou, C.-Y., *J. Phys. Chem.* **111** (2007) 18731.
58. Ardizzone, S., Bianchi, C. L., Cappelletti, G., Porta, F., *J. Catal.* **227** (2004) 470.
59. Zhu, L., Xiao, F.-S., Zhang, Z., Sun, Y., Han, Y., Qiu, S., *Catal. Today.* **68** (2001) 209.
60. Khodakov, A., Yang, J., Su, S., Iglesia, E., Bell, A. T., *J. Catal.* **177** (1998) 343.